Localized States due to Expulsion of Resonant Impurity Levels from the Continuum in Bilayer Graphene

V. V. Mkhitaryan and E. G. Mishchenko

Phys. Rev. Lett. **110**, 086805 — Published 20 February 2013

DOI: 10.1103/PhysRevLett.110.086805

Localized states due to expulsion of resonant impurity levels from the continuum in bilayer graphene

V. V. Mkhitaryan and E. G. Mishchenko
Department of Physics and Astronomy, University of Utah, Salt Lake City, UT 84112, USA

Anderson impurity problem is considered for a graphene bilayer subject to a gap-opening bias. In-gap localized states are produced even when the impurity level overlaps with the continuum of band electrons. The effect depends strongly on the polarity of the applied bias as long as hybridization with the impurity occurs within a single layer. For an impurity level inside the conduction band a positive bias creates the new localized in-gap state. A negative bias does not produce the same result and leads to a simple broadening of the impurity level. The implications for transport are discussed including a possibility of gate-controlled Kondo effect.

PACS numbers: 73.22.Pr,73.20.At,73.22.Dj

Introduction. Electronic properties of graphene are affected by short-range scatterers (for the review see Ref. [1]). Remarkably, these properties significantly depend on the character of disorder [2]. It has been demonstrated that the limit of *strong* scattering is realized via resonances occurring for vacancies [3–5] and adsorbed atoms [6–10]. Such resonances lead to the modification of the bare spectrum near the charge neutrality point and strongly affect the transport properties.

Moreover, the localized impurity levels in a graphene host could potentially result in a formation of local magnetic moments [11–14]. This situation is of a special interest as it opens up a perspective of controlled switching of the local moments by gating. As far as the transport properties are concerned the local magnetic moments famously lead to the Kondo effect. The band structure of the monolayer graphene makes this effect different than that in normal metals [16–18]. On one hand, narrowing of the impurity level due to the vanishing density of states (DOS) in graphene, $\rho(E_F) \propto |E_F|^\alpha$, facilitates the formation of a local moment near the charge neutrality point. On the other hand, the low DOS disfavors the Kondo resonance and results in the suppression of the Kondo temperature when $E_F \to 0$. In case of non-interacting electrons, $\alpha = 1$, the suppression is power-law. If the effects of electron-electron renormalization of the spectrum are included, so that $\alpha < 1$, the Kondo temperature is suppressed exponentially.

The theory of resonant impurity states in *bilayer* graphene has received much less attention despite its greater technological potential. The most important property of bilayer graphene to this extent is its gap tunable by external bias [19–21]. It is therefore important to elucidate how strongly the gap is affected by the disorder, which generally tends to smear the gap. For short-range impurity potential there exist "tail-states" with DOS decaying exponentially from the band edge [22–24]. Numerical studies also indicate the onset of well-defined midgap peaks in the presence of resonant impurities [10].

In the present paper we analyze the effect of the Anderson impurity hybridized with the band electrons of bilayer graphene host. We demonstrate that a single impurity level with energy ε_0 induces a localized in-gap state. This is a rather trivial statement whenever ε_0 falls within the (gate-induced) bandgap. More interestingly, we find that the in-gap state appears even if the impurity level

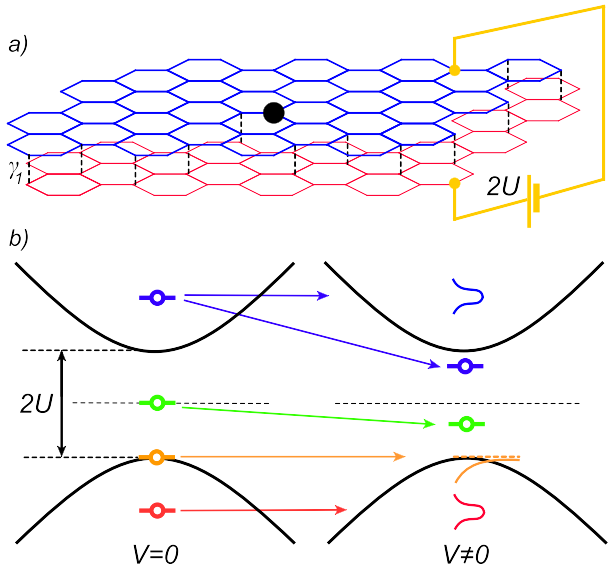

FIG. 1: a) Bilayer graphene subject to the gap-opening bias $2U$. The resonant impurity (black circle) is hybridized with π-electrons of a carbon atom in the upper layer. Tunneling γ_1 is indicated by the vertical dashed lines. b) Band structure of the system for different impurity energies ε_0. The left picture corresponds to a zero hybridization amplitude V. The right one illustrates the modification of the spectrum for finite couplings V and positive bias $U > 0$. The level with $\varepsilon_0 > U$ (blue) broadens due to coupling to the band electrons while generating an additional in-gap state. The level originally positioned inside the gap (shown with green for a specific case $\varepsilon_0 = 0$) remains localized but is renormalized towards lower energies. States overlapping with the valence band $\varepsilon_0 < -U$ (red) are broadened without generating any additional in-gap states. The level at the top of the valence band (orange) leads to a square-root singularity in the density of states.

sits inside the *continuum* of itinerant states, i.e. above or below the bandgap, depending on the *polarity* of the applied interlayer bias. We consider a realistic bilayer setup, shown in Fig. 1, of an impurity sitting on top of the upper layer. Consider the case of a positive applied bias $2U/e$ as shown in the picture ($-e$ is the electron charge). We emphasize that in this case the localized state appears *no matter how high* the impurity level ε_0 is above the charge neutrality point. To the contrary, the impurity state overlapping with the valence band, $\varepsilon_0 < -U$, does not generate a localized state. It simply acquires a finite width (and the energy renormalization) from the interaction with the valence band states.

The localized states of the similar nature that appear due to hybridization with an impurity level are known to occur in various systems. In a one-dimensional band with a finite bandwidth a pair of states split off near both band edges [26]. In conventional s-wave superconductors similar bound states are long known [27, 28]. However, they lie extremely close to the superconducting gap (typically within $\sim 10^{-3}$ of its width), and thus are hardly discernable against the divergent superconducting DOS. In contrast, in bilayer graphene it is possible to "place" the localized state virtually *anywhere* within the bandgap simply by controlling the applied bias. In particular, this can lead to the emergence of a local magnetic moment and a formation of the Kondo resonance, more robust than in a monolayer, even when the bare impurity level ε_0 is *above* the Fermi level.

Anderson impurity in bilayer graphene. The low-energy Hamiltonian of bilayer graphene is a 4×4 matrix in layer/sublattice space [29]. If in addition the energies of interest are less than the interlayer tunneling rate the Hamiltonian could be reduced further to the 2×2 matrix acting on the layer index. In the presence of a gap-opening electrostatic potential difference $2U$ such Hamiltonian has the form [1, 29],

$$\hat{H}(\mathbf{p}) = \frac{1}{2m}\left([p_x^2 - p_y^2]\hat{\sigma}_x + 2p_x p_y \hat{\sigma}_y\right) + U\hat{\sigma}_z, \qquad (1)$$

where $\hat{\sigma}_i$ are the Pauli matrices, and $\mathbf{p}$ is the electron quasimomentum. The effective mass $m = \gamma_1/2v^2 = 0.03m_0$ is determined by the interlayer coupling, $\gamma_1 = 0.35$ eV, and the Dirac velocity, $v = 10^6$ m/s. This Hamiltonian acts on the two-component wavefunction, $\hat{\psi}^\dagger_{\mathbf{p}} = (\psi^*_{1\mathbf{p}}, \psi^*_{2\mathbf{p}})$, with $\psi_{\sigma\mathbf{p}}$ referring to the amplitudes on upper ($\sigma = 1$) and lower ($\sigma = 2$) layers. The total Hamiltonian of the system in the second quantization representation is

$$\mathcal{H} = \sum_{\mathbf{p}} \hat{\psi}^\dagger_{\mathbf{p}} \hat{H}(\mathbf{p}) \hat{\psi}_{\mathbf{p}} + \varepsilon_0 d^\dagger d + V\sum_{\mathbf{p}} (\psi^\dagger_{1\mathbf{p}} d + d^\dagger \psi_{1\mathbf{p}}), \quad (2)$$

where the second term describes the localized level and the last term defines the hybridization of this level with band-electrons in the upper layer only. This choice, while not of principal importance for the calculations, ensures the asymmetry with respect to the polarity of U as we show below. The properties of the localized electrons are most conveniently described by its Green's functions,

$$D(t) = -i\langle T d(t) d^\dagger(0)\rangle. \qquad (3)$$

This function satisfies the equation which follows from Eq. (2). In the energy representation,

$$(E - \varepsilon_0) D(E) = 1 + V\mathcal{G}_1(0, E). \qquad (4)$$

The mixed Green's function in the latter equation is defined according to

$$\mathcal{G}_\sigma(\mathbf{r}, t) = -i\langle T\psi_\sigma(\mathbf{r}, t) d^\dagger(0)\rangle \qquad (5)$$

and satisfies the equation

$$(E - \hat{H})_{\sigma\sigma'} \mathcal{G}_{\sigma'}(\mathbf{r}, E) = V\delta(\mathbf{r})\delta_{\sigma 1} D(E). \qquad (6)$$

The two equations (4) and (6) form a closed system that readily yields the solution,

$$D(E) = \frac{1}{E - \varepsilon_0 - V^2 G^{(0)}_{11}(E)}, \qquad (7)$$

where we introduced the Green's function of free band electrons, $\hat{G}^{(0)}(E) = \sum_{\mathbf{p}} [E - \hat{H}(\mathbf{p}) + i\eta\ \mathrm{sign} E]^{-1}$. In what follows we are mostly interested in the gapped region, $-U < E < U$, where after simple calculations [30] we obtain $G^{(0)}_{11}(E) = -\frac{m}{2}\frac{E+U}{\sqrt{U^2 - E^2}}$. Remarkably, in this region there exists a bound state which emerges as a simple pole of the Green's function $D(E)$, Eq. (7). Its energy satisfies the relation

$$E - \varepsilon_0 + \Gamma\sqrt{\frac{U+E}{U-E}} = 0. \qquad (8)$$

Here we introduced the parameter, $\Gamma = mV^2/2$, whose meaning is the inverse lifetime of the original impurity level high above the gap, $E \gg U$. Remarkably, the equation (8) is asymmetric with respect to the sign of the applied bias U. Let us concentrate on the case of positive bias $U > 0$ below. The generalization to the opposite case is almost evident and will be discussed later. It is easy to see that Eq. (8) has a true in-gap bound state solution, $\widetilde{\varepsilon}$, for *any* impurity level such that $\varepsilon_0 > -U$. Fig. 1 illustrates the energy spectrum of the system for various values of ε_0. The most trivial case is realized when ε_0 falls within the bandgap $-U < \varepsilon_0 < U$. Here the energy of the resulting localized state is lowered by the hybridization, $\widetilde{\varepsilon} < \varepsilon_0$. Moreover, impurity level inside the positive energy band $\varepsilon_0 > U$ *always* creates an in-gap localized state, regardless of how large ε_0 and/or how narrow the gap is.

The effect of the impurity level is two-fold. First, its interaction with band electrons broadens its density of

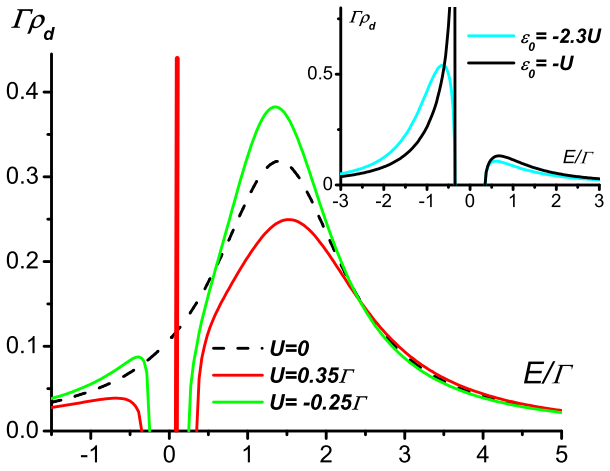

FIG. 2: a) Dimensionless density of states (scaled with the coupling strength Γ) of the d-electrons plotted in units of $1/\Gamma$ for $\Gamma = \gamma_1/2$, $\varepsilon_0 = 0.7\gamma_1$, and three different values of bias U: zero bias (black dashed line), positive bias (red), negative bias (green). The bound in-gap state appears as a sharp peak for $U > 0$, but not for $U < 0$. Inset: development of a square-root singularity when the impurity level is approaching the top of the valence band from the inside of it.

states. This could be readily seen from Eq. (7) with $|E| > U$, where the self energy of the d-state becomes purely imaginary, $G_{11}^{(0)}(E) = -i\frac{m}{2}\frac{E+U}{\sqrt{E^2-U^2}}$. The density of states of the impurity level $\rho_d(E)$ is modified from the simple Lorentzian, which is the case when $U = 0$:

$$\rho_d(E) = -\frac{\Im D_R(E)}{\pi} = \frac{\Gamma\sqrt{E^2-U^2}/\pi}{(E-\varepsilon_0)^2|E-U| + \Gamma^2|E+U|}. \tag{9}$$

Fig. 2 shows the density of impurity states for different values of the gap. The second feature is the appearance of the delta-function peak, corresponding to the new localized state, Eq. (8), also indicated in Fig. 2. The total area under any curve is $\int \rho_d(E)dE = 1$. In evaluating this area one notices that the in-gap peak in $\rho_d(E)$ has a spectral weight smaller than unity:

$$\rho_d(E) = \frac{(U-\widetilde{\varepsilon})^{3/2}(U+\widetilde{\varepsilon})^{1/2}}{(U-\widetilde{\varepsilon})^{3/2}(U+\widetilde{\varepsilon})^{1/2} + U\Gamma}\,\delta(E-\widetilde{\varepsilon}). \tag{10}$$

The remaining spectral weight that completes the total weight of the in-gap state to the unity comes from the band electrons. This can be verified by calculating the band electron Green's function, $G_{\sigma\sigma'}(\mathbf{r},\mathbf{r}',t) = -i\langle T\psi_\sigma(\mathbf{r},t)\psi^\dagger_{\sigma'}(\mathbf{r}',0)\rangle$, accomplished by constructing a system of coupled equations similar to Eqs. (4) and (6).

Impurity levels overlapping with the valence band. When the impurity level resides inside the lower continuum of band states, $\varepsilon_0 < -U$, the broadening of the level *is not* accompanied by the creation of an in-gap state, see Fig. 1. Far from the band edge $-\varepsilon_0 \gg U$ the lineshape is a simple Lorentzian but is distorted as ε_0 moves closer to the edge. At $\varepsilon_0 = -U$ the density of states develops a singularity $\rho_d \sim \Gamma^{-1}\sqrt{U/|E+U|}$. Both these cases are shown in the inset on Fig. 2.

The asymmetry between the positive and negative energies ε_0 and the sensitivity to the sign of the external bias is a manifestation of breaking of the symmetry between the two layers by the impurity position. If the impurity particle is hybridized equally with both monolayers the symmetry is restored and the in-gap bound state is always present. It is found from an equation similar to Eq. (8), where the square root is replaced with $2E/\sqrt{U^2-E^2}$.

4×4 *bilayer Hamiltonian.* In the previous discussion we utilized the simplified two-band model, which is usually justified when the typical energies are small compared with the interlayer tunneling, E, $U \ll \gamma_1$. We are now going to discuss the new qualitative features that the inclusion of all four π-electron bands leads to. The full four-band Hamiltonian is a 4×4 matrix [29],

$$\hat{H}(\mathbf{p}) = \begin{pmatrix} U & vp_+ & 0 & 0 \\ vp_- & U & \gamma_1 & 0 \\ 0 & \gamma_1 & -U & vp_- \\ 0 & 0 & vp_+ & -U \end{pmatrix}, \tag{11}$$

where $p_\pm = p_x \pm ip_y$. The first two rows/columns of Eq. (11) refer to the two sublattices in the upper graphene layer and the last two to the lower layer. The formal expression for the total Hamiltonian of the system, Eq. (1), remains unchanged with the exception of the dimensionality of spinors $\hat{\psi}_\mathbf{p}$. The effect of hybridization is the strongest when the impurity sits on a carbon atom belonging to the *first* sublattice – the one not directly coupled by tunneling γ_1 to the second layer. A rather peculiar situation of an impurity residing on the other sublattice of the first layer is discussed below.

The pole of Eq. (7) still defines the bound state with the corresponding self-energy given by the integral of the Green's function over momentum,

$$G_{11}^{(0)}(E) = \frac{U-E}{8\pi v^2}\ln\frac{D^4}{(U^2-E^2)(\gamma_1^2+U^2-E^2)} - \frac{\gamma_1^2(U+E)+2UE(U-E)}{4\pi v^2\gamma_1 U\sqrt{1-E^2/\widetilde{U}^2}}\left(\frac{\pi}{2}+\tan^{-1}\frac{E^2+U^2}{\gamma_1 U\sqrt{1-E^2/\widetilde{U}^2}}\right). \tag{12}$$

One of the consequences of the expanded Halimtonian (11) is that the true gap $\widetilde{U} = \gamma_1 U/\sqrt{\gamma_1^2 + 4U^2}$ is found at a finite momentum. Since $\widetilde{U}$ is slightly less than U, the logarithmic term in Eq. (12) is cut-off and represents a non-significant renormalization of ε_0. The most significant difference obtained in the 4×4 model is the behavior at $E \sim -\widetilde{U}$, where $G_{11}^{(0)}(E)$ changes sign and therefore *allows* the in-gap state solution expelled from the inside of the *valence* band, $\varepsilon_0 < -U$, situation forbidden by Eq. (8). Such states are residing very close to the top of the band as the overall effect is rather weak. For the binding energy we obtain the expression,

$$\widetilde{\varepsilon} + \widetilde{U} = \frac{8\Gamma^2 U^5}{\gamma_1^4 (|\varepsilon_0| - \widetilde{U})^2}, \tag{13}$$

applicable as long as $|\varepsilon_0| - \widetilde{U} \gg \Gamma U^2/\gamma_1^2$.

Let us now turn to the impurity sitting on top of an atom belonging to the *second* (directly coupled by tunneling to the bottom layer) sublattice. In this case the self-energy in Eq. (7) is given by $G_{22}^{(0)}(E)$ instead of $G_{11}^{(0)}(E)$. The former is determined by expression similar to Eq. (12) where the term $\gamma_1^2(U+E)$ in the numerator of the second term is set to zero. There are two notable consequences of this change. First, all bound solutions for the impurity overlapping with the conduction band, $\varepsilon_0 > U$, completely *disappear*. The only non-trivial states are those emerging from the valence band. Second, such states are expelled stronger than in the case considered in the previous paragraph. This is reflected in the increased binding energy, which is given by Eq. (13) multiplied by the extra factor 4.

It is also straightforward to address a general case of an impurity hybridized with both sublattices of the top layer, with arbitrary amplitudes V_1 and V_2. The equation (7) still holds provided that the self-energy is replaced with $V_1^2 G_{11}^{(0)}(E) + V_2^2 G_{22}^{(0)}(E)$. Note the absence of the cross-terms at coinciding points, $G_{12}^{(0)}(E) = 0$. The more general situation, therefore, interpolated between the case $V_2 = 0$ considered throughout the paper and the case $V_1 = 0$ discussed in the previous paragraph. The hybridization amplitude V_1 now defines how efficiently a localized state appears when the level overlaps with the conduction band, and the amplitude V_2 controls the (weak) splitting of the state off the top of the valence band whenever the impurity level happens to be inside it.

Gate-controlled Kondo effect via formation of a local magnetic moment. A direct inclusion of the spin degree of freedom in the Hamiltonian (2) does not change the above physical picture unless the electron-electron interaction is taken into account. In the presence of the spin degeneracy, this interaction is often described by the on-site Hubbard repulsion, which under some conditions can cause a magnetic instability [31]. Such a description, however, might not be adequate for the in-gap states found above. Indeed, as evident from Eq. (10), a significant fraction of the spectral weight comes from the evanescent band states, in particular, when $\widetilde{\varepsilon}$ is close to the band edges, $\pm U$. We consider the most intriguing situation of an impurity level high in the conduction band $\varepsilon_0 \gg U$, so that the in-gap state is close to U. To estimate the magnitude of the Coulomb charging energy, we note that the radius of this state is $R \sim [2m(U-\tilde{\varepsilon})]^{-1/2}$. In turn, the binding energy can be found from Eq. (8) to be $U - \tilde{\varepsilon} \simeq 2\Gamma^2 U/(\varepsilon_0 - U)^2$. Therefore the charging energy is $E_c \simeq 2e^2/R \simeq e^2\Gamma\sqrt{mU}/\varepsilon_0$. The condition for the formation of a well-defined magnetic moment in the n-doped bilayer (with the Fermi energy $E_F > U$) is that the double occupancy of the in-gap state is forbidden, $E_c > E_F - U$. In terms of the gap-opening bias, this happens when $U > (E_F - U)^2 \varepsilon_0^2/4E_B\Gamma^2$, where we introduce the Bohr energy, $E_B \approx 1.47$ eV. As seen from this estimate higher amplitudes Γ favor the Kondo effect. In particular, for $U = 100$ meV and $E_F - U = 50$ meV it would be required that $\Gamma > \varepsilon_0/15$. Under these conditions the gate-controlled Kondo effect can potentially be observed in bilayer graphene, where one has the additional benefit of a finite DOS, in contrast to a monolayer. We emphasize that such a gate-controlled formation of magnetic moment differs substantially from the proposal of Ref. [32], as the latter is stipulated by the dependence of ε_0 on the applied bias.

Conclusion. An important difference between the above found resonant bound states with the previously predicted bound states due to short-range impurities [22, 23] or vacancies [25] is that in our case the emerging states can reside anywhere inside the gap, not just close to the band edges or, as is the case for vacancies, at zero energy. Note that zero-energy states, quasi-localized in the gapless bilayer graphene unsurprisingly develop into truly localized states for any finite bias. In our case, in contrast, the impurity state can be at a finite energy ϵ_0 above the gap and still result in the in-gap localized state. From a practical standpoint, controlled doping with atoms or molecules appears to be more plausible than with vacancies.

Wide range for the hybridization energies for a number of impurities (H, CH_3, OH, F) has been reported from the first principles from $W \sim 0.7$ eV in Ref. 9 to $W \sim 5$ eV in Ref. 7. Within the effective Dirac description this corresponds to $V \sim (3^{3/4}a/2\hbar)W$, where the interatomic distance $a = 1.42$ Å. Using this estimate, $\Gamma \sim 10 - 250$ meV. Due to this large value of Γ, the depth of the induced in-gap bound state is comparable with U for values of ε_0 as large as a few Γ. In addition to the above discussed Kondo effect, the potential experimental implications include sub-gap gate-dependent optical absorption, as well as the variable-range hopping transport via the impurity band, which would form in the presence of a finite density of impurities.

Thus far we have neglected the effect of band electron-electron interactions. Theoretical studies [33–39] predicted various broken symmetry states when the electron density is at the charge neutrality point, with the induced gaps, however, not exceeding a few meV. Some evidence confirming these predictions, has also been observed experimentally [40–42]. Nonetheless, since typical bias-induced gaps of interest to us are at least an order of magnitude higher, this modification of the low-energy spectrum due to electron-electron interactions should not affect the above physical picture.

Useful discussions with M. Raikh and O. Starykh are gratefully acknowledged. The work was supported by the Department of Energy, Office of Basic Energy Sciences, Grant No. DE-FG02-06ER46313.

[1] A.H. Castro Neto, F. Guinea, N.M.R. Peres, K.S. Novoselov, and A.K. Geim, Rev. Mod. Phys. 81, 109 (2009).
[2] P. M. Ostrovsky, I. V. Gornyi, and A. D. Mirlin, Phys. Rev. B **74**, 235443 (2006).
[3] N. M. R. Peres, F. Guinea, and A. H. Castro Neto, Phys. Rev. B **73**, 125411 (2006).
[4] V. M. Pereira, F. Guinea, J. M. B. Lopes dos Santos, N. M. R. Peres, and A. H. Castro Neto, Phys. Rev. Lett. **96**, 036801 (2006).
[5] V. M. Pereira, J. M. B. Lopes dos Santos, and A. H. Castro Neto, Phys. Rev. B **77**, 115109 (2008).
[6] T. O. Wehling, S. Yuan, A. I. Lichtenstein, A. K. Geim, and M. I. Katsnelson, Phys. Rev. Lett. **105**, 056802 (2010).
[7] J. P. Robinson, H. Schomerus, L. Oroszlany, and V. I. Falko, Phys. Rev. Lett. **101**, 196803 (2008).
[8] T. Stauber, N. M. R. Peres, and F. Guinea, Phys. Rev. B **76**, 205423 (2007).
[9] T. O. Wehling, M. I. Katsnelson, and A. I. Lichtenstein, Phys. Rev. B **80**, 085428 (2009).
[10] A. Ferreira, J. Viana-Gomes, J. Nilsson, E. R. Mucciolo, N. M. R. Peres, and A. H. Castro Neto, Phys. Rev. B **83**, 165402 (2011).
[11] B. Uchoa, V. N. Kotov, N. M. R. Peres, and A. H. Castro Neto Phys. Rev. Lett. **101**, 026805 (2008).
[12] B. Uchoa, L. Yang, S.-W. Tsai, N. M. R. Peres, and A. H. Castro Neto, Phys. Rev. Lett. **103**, 206804 (2009).
[13] B. Uchoa, T. G. Rappoport, and A. H. Castro Neto, Phys. Rev. Lett. **106**, 016801 (2011).
[14] C. Li, J.-X. Zhu, and C.S. Ting, arXiv:1106.5827
[15] P. S. Cornaglia, G. Usaj, and C. A. Balseiro, Phys. Rev. Lett. **102**, 046801 (2009).
[16] K. Sengupta and G. Baskaran, Phys. Rev. B **77**, 045417 (2008).
[17] C. R. Cassanello and E. Fradkin, Phys. Rev. B **53**, 15079 (1996).
[18] M. Vojta, L. Fritz, and R. Bulla, Europhys. Lett. **90**, 27006 (2010).
[19] A. B. Kuzmenko, I. Crassee, D. van der Marel, P. Blake, and K. S. Novoselov, Phys. Rev. B **80**, 165406 (2009).
[20] Y. Zhang, T.-T. Tang, C. Girit, Z. Hao, M. C. Martin, A. Zettl, M.F. Crommie, Y. R. Shen, and F. Wang, Nature **459**, 820 (2009).
[21] K. F. Mak, C. H. Lui, J. Shan, and T. F. Heinz, Phys. Rev. Lett. **102**, 256405 (2009).
[22] J. Nilsson and A. H. Castro Neto, Phys. Rev. Lett. **98**, 126801 (2007).
[23] H. P. Dahal, A. V. Balatsky, and J.-X. Zhu, Phys. Rev. B **77**, 115114 (2008).
[24] V. V. Mkhitaryan and M. E. Raikh, Phys. Rev. B **78**, 195409(2008).
[25] E. V. Castro, M. P. Lopez-Sancho, and M. A. H. Vozmediano, Phys. Rev. Lett. **104**, 036802 (2010).
[26] G. Mahan, *Many Particle Physics* (Plenum, New York, 2000).
[27] K. Machida and F. Shibata, Prog. Theor. Phys. **47**, 1817 (1972).
[28] H. Shiba, Prog. Theor. Phys. **50**, 50 (1973).
[29] E. McCann and V.I. Fal'ko, Phys. Rev. Lett. **96**, 086805 (2006).
[30] Here we take into account K and K' valley degeneracy with the extra factor 2. Considering this degeneracy explicitly in the Hamiltonian Eq. (1) leads to the same conclusion.
[31] A. C. Hewson, *The Kondo Problem To Heavy Fermions* (Cambridge University Press, Cambridge, UK, 1997).
[32] M. Killi, D. Heidarian, and A. Paramekanti, New J. Phys. **13**, 053043 (2011).
[33] H. Min, G. Borghi, M. Polini, and A. H. MacDonald, Phys. Rev. B **77**, 041407(R) (2008).
[34] K. Sun, H. Yao, E. Fradkin, and S. A. Kivelson, Phys. Rev. Lett. **103**, 046811 (2009).
[35] R. Nandkishore and L. Levitov, Phys. Rev. Lett. **104**, 156803 (2010).
[36] O. Vafek and K. Yang, Phys. Rev. B **81**, 041401 (2010).
[37] Y. Lemonik, I. L. Aleiner, C. Toke, and V. I. Fal'ko, Phys. Rev. B **82**, 201408 (2010).
[38] F. Zhang, J. Jung, G. A. Fiete, Q. Niu, and A. H. MacDonald, Phys. Rev. Lett. **106**, 156801 (2011).
[39] E. V. Gorbar, V. P. Gusynin, V. A. Miransky, and I. A. Shovkovy, Phys. Rev. B **85**, 235460 (2012).
[40] A. S. Mayorov, D. C. Elias, M. Mucha-Kruczynski, R. V. Gorbachev, T. Tudorovskiy, A. Zhukov, S. V. Morozov, M. I. Katsnelson, V. I. Fal'ko, A. K. Geim, and K. S. Novoselov, Science **333**, 860 (2011).
[41] F. Freitag, J. Trbovic, M. Weiss, and C. Schonenberger, Phys. Rev. Lett. **108**, 076602 (2012).
[42] J. Velasco Jr., L. Jing, W. Bao, Y. Lee, P. Kratz, V. Aji, M. Bockrath, C. N. Lau, C. Varma, R. Stillwell, D. Smirnov, F. Zhang, J. Jung, and A. H. MacDonald, Nat. Nanotechnology 7, 156 (2012).